B4GALT6 regulates astrocyte activation during CNS inflammation

Lior Mayo[1], **Sunia A. Trauger**[2], **Manon Blain**[3], **Meghan Nadeau**[1], **Bonny Patel**[1], **Jorge I. Alvarez**[4], **Ivan D. Mascanfroni**[1], **Ada Yeste**[1], **Pia Kivisäkk**[1], **Keith Kallas**[1], **Benjamin Ellezam**[5], **Rohit Bakshi**[1], **Alexandre Prat**[4], **Jack P. Antel**[3], **Howard L. Weiner**[1], and **Francisco J. Quintana**[1],*

[1]Center for Neurologic Diseases, Brigham and Women's Hospital, Harvard Medical School, Boston, MA, USA

[2]FAS Center for Systems Biology, Harvard University, Boston, MA, USA

[3]Neuroimmunology Unit, Montreal Neurological Institute, Department of Neurology and Neurosurgery, McGill University, Montreal, QC, Canada

[4]Neuroimmunology Research Lab, Center for Excellence in Neuromics, Department of Neuroscience, Université de Montréal, Montréal, QC, Canada

[5]Department of Pathology, Centre de Recherche du Centre Hospitalier de, l'Université de Montréal and Faculty of Medicine, Université de Montréal, Montréal, QC, Canada

Abstract

Astrocytes play complex roles in the response to trauma, infection or inflammation in the central nervous system (CNS). Thus, it is important to characterize the mechanisms regulating astrocyte function, as well as potential targets for the therapeutic modulation of astrocyte activity. Here we report that lactosylceramide (LacCer) levels are up-regulated in the CNS during chronic experimental autoimmune encephalomyelitis (EAE), an experimental model of multiple sclerosis (MS). We found that LacCer synthesized by β-1,4-galactosyltransferase 6 (B4GALT6) in astrocytes acts in an autocrine manner to trigger transcriptional programs that promote the recruitment and activation of CNS-infiltrating monocytes and microglia, and neurodegeneration. We also detected increased *B4GALT6* expression and LacCer levels in CNS MS lesions. Finally, the inhibition of LacCer synthesis suppressed local CNS innate immunity and neurodegeneration in EAE, and interfered with the activation of human astrocytes *in vitro*. Thus, B4GALT6 is a potential therapeutic target for MS and other neuroinflammatory disorders.

Astrocytes are the most abundant cells in the central nervous system (CNS). Under normal conditions astrocytes modulate synaptic activity, and provide nutrients and support needed for neuronal survival [1–4]. In the context of neuroinflammation, astrocytes control CNS infiltration by peripheral pro-inflammatory leukocytes [5–8] and are suggested to regulate the activity of microglia, oligodendrocytes and cells of the adaptive immune system [9]. Thus, it is important to characterize the mechanisms regulating astrocyte activation during CNS inflammation, as well as potential targets for the therapeutic modulation of astrocyte activity.

Multiple sclerosis (MS) is a chronic demyelinating autoimmune disease of the CNS. In most patients, MS initially presents a relapsing-remitting clinical course (relapsing-remitting MS, RRMS) that is followed by a progressive phase (secondary progressive MS, SPMS) characterized by a continued and irreversible accumulation of disability in which available treatments show limited efficacy [10]. Recent findings suggest that the local CNS innate immune response drives disease progression in SPMS [9,11,12]. Thus, we investigated the role of astrocytes in CNS autoimmunity using an experimental model that recapitulates several aspects of SPMS.

Here we report that lactosylceramide (LacCer), produced by the enzyme B4GALT6 in astrocytes during chronic CNS inflammation, acts in an autocrine manner to promote inflammation and neurodegeneration. We also found up-regulated expression of *B4GALT6* and increased LacCer levels in CNS lesions from MS patients. These findings identify B4GALT6 in astrocytes as a driver of chronic CNS inflammation, and also as a potential therapeutic target for the treatment of MS and other neuroinflammatory disorders.

Results

LacCer synthases control CNS inflammation and neurodegeneration

Experimental autoimmune encephalomyelitis (EAE) constitutes a useful experimental model of MS, but different aspects of the disease are modeled in each mouse strain. C57BL/6 mice immunized with $MOG_{35–55}$ develop a monophasic EAE that resembles a single attack during RRMS. Immunization of non-obese diabetic (NOD) mice with $MOG_{35–55}$, however, results in an acute attack (acute phase) followed by a phase of progressive and irreversible accumulation of neurological impairment (progressive phase) that resembles SPMS [13,14].

We found that F1 hybrid mice derived from breeding NOD and C57BL/6 mice develop a chronic progressive form of EAE (Supplementary Fig. 1). Thus, to study the role of astrocytes during CNS inflammation we analyzed the course of EAE in F1 NOD C57BL/6 GFAP-HSV-TK hybrid mice, in which reactive astrocytes can be depleted by Ganciclovir (GCV) administration (Supplementary Fig. 2a). In accordance with previous findings in C57BL/6 mice [7,8], the depletion of reactive astrocytes during the acute phase resulted in EAE worsening (Fig. 1a). However, astrocyte depletion during the progressive phase led to a significant amelioration of EAE (Fig. 1a). Moreover, although reactive astrocyte depletion in acute EAE results in increased monocyte and T-cell recruitment to the CNS [5,8], depletion during the progressive phase of EAE decreased leukocyte infiltration in the CNS (Supplementary Fig. 2b) but did not affect the peripheral T-cell response (Supplementary

Figs. 2c,d). Of note, although GCV administration might potentially deplete neural progenitor cells (NPCs) in NOD C57BL/6 GFAP-HSV-TK hybrid mice, NPCs show protective effects in EAE [15,16]. Thus, these data suggest that depletion of reactive astrocytes is responsible for the amelioration of EAE.

To study the regulation of astrocyte activity we isolated astrocytes from naïve NOD mice, or during the acute and the progressive phases of EAE (Supplementary Fig. 3), and analyzed their transcriptome with Nanostring nCounter arrays (Supplementary Table 1). We detected mRNA expression profiles linked to different stages of NOD EAE and identified a set of genes up-regulated during the progressive phase (Fig. 1b). One of the genes whose expression was associated with progressive NOD EAE was *b4galt6*, a LacCer synthase [17]. *B4galt6* up-regulation in astrocytes, but not microglia, was validated by qPCR (Fig. 1c). Further validation detected B4GALT6 expression in white matter GFAP[+] astrocytes, but not in gray matter, perivascular glia limitans, or in nestin[+] neural progenitors (Supplementary Figs. 4a,b). We also detected the up-regulation of β-1,4-galactosyltransferase 5 (B4GALT5), which together with B4GALT6 are the only members of the B4GALT family with LacCer synthase activity [17] (Supplementary Fig. 4c). Indeed, in agreement with the LacCer synthase activity of B4GALT5 and B4GALT6 (B4GALT5/6), we detected increased LacCer levels in the CNS during the progressive phase of NOD EAE (Fig. 1d).

We then investigated the effects of LacCer on CNS inflammation. LacCer administration worsened EAE in C57BL/6 and NOD mice (Figs. 1e,f), but could not induce EAE or astrocyte activation *in vivo* in the absence of MOG immunization (Supplementary Fig. 5a). Of note, LacCer administration did not affect the T-cell response (Supplementary Figs. 5b–e).

To further investigate the role of LacCer in the progressive phase of NOD EAE we inhibited its synthesis using the B4GALT5/6-specific inhibitor D-*threo*-1-phenyl-2-decanoylamino-3-morpholino-1-propanol (PDMP) [17] (Fig. 1g). Daily PDMP administration initiated 40 days after EAE induction decreased CNS LacCer levels (Fig. 1h) and suppressed disease progression in terms of clinical score, demyelination and axonal loss (Fig. 1i,j). PDMP did not affect the T-cell response (Supplementary Figs. 5f–i). Taken together, these data suggest that LacCer produced by B4GALT5/6 plays a detrimental role in CNS inflammation.

B4GALT5/6 inhibition suppresses astrocyte activation during EAE

LacCer has been suggested to promote pathology during experimental spinal cord injury [18]. Thus, we studied the effects of B4GALT5/6 inhibition on the transcriptional program of astrocytes isolated from vehicle- or PDMP-treated NOD mice during the progressive phase of EAE (day 100). Our unbiased analysis identified two sets of genes: genes down-regulated during EAE and up-regulated by PDMP, and genes up-regulated during EAE and down-regulated by PDMP (clusters 1 and 2 in Fig. 2a, respectively). Cluster 2 included several genes associated with EAE and MS pathology: *ccl2* (recruitment of monocytes to the CNS) [19–21], *ccl5* and *cxcl10* (recruitment of peripheral immune cells to the CNS), IL-1β (*il1b*), osteopontin (*opn*), nitric oxide synthase (*nos2*), MHC-II (*H2-Aa*) and vimentin (*vim*). The suppressive effects of PDMP on the expression of representative genes included in cluster 2 were validated by qPCR (Fig. 2b). Additional support for the role of B4GALT6 in

regulating the expression of genes associated with CNS pathology was provided by the co-expression of B4GALT6 with CCL2 and iNOS in GFAP$^+$ astrocytes (Supplementary Fig. 6).

Moreover, since astrocytes are reported to regulate de- and re-myelination [9,22], we analyzed the expression of genes linked to the control of this process by astrocytes (Supplementary Table 2 and Fig. 2c). B4GALT5/6 inhibition by PDMP reduced the expression of demyelination-associated genes while it increased the expression of remyelination-associated genes (Fig. 2c). Collectively, these data demonstrate that B4GALT5/6 controls astrocyte activation during EAE.

To identify the molecular mechanisms mediating the effects of B4GALT5/6 blockade on the transcriptional response of astrocytes during EAE, we searched the promoter sequence of the genes included in clusters 1 and 2 for the enrichment of specific transcription factor binding sites. We found that genes included in cluster 2, whose expression was suppressed by B4GALT5/6 inhibition, were enriched for interferon-sensitive response elements (ISREs) (P=4.83×10^{-6}) and NF-κB response elements (P=9.99×10^{-6}). Indeed, *irf1* and *relB* expression was up-regulated during EAE and decreased by PDMP treatment (Fig. 2d,e). Hence, these results suggest that B4GALT5/6 controls NF-κB and IRF-1 activation during CNS inflammation.

LacCer produced by B4GALT6 acts in an autocrine manner to boost astrocyte activation

To investigate whether LacCer produced by B4GALT5/6 acts directly on astrocytes to regulate their activity, we studied the effects of B4GALT5/6 inhibition and LacCer supplementation on the transcriptional response of primary astrocytes to activation. B4GALT5/6 inhibition suppressed the response of astrocytes to stimulation with lipopolysaccharide and interferon-γ (LPS/IFNγ) (Figs. 3a and Supplementary Fig. 7a). Conversely, supplementation with exogenous LacCer boosted the astrocyte response to LPS/IFNγ suggesting that LacCer synthesized by B4GALT5/6 acts on an autocrine manner to promote astrocyte activation (Figs. 3a and Supplementary Fig. 7a). Consistent with this interpretation, exogenous LacCer overcame the suppressive effects of PDMP on astrocyte activation (Figs. 3a and Supplementary Fig. 7a). Similar effects of PDMP and LacCer were found on astrocytes activated with IL-1β, poly(I:C), or IFNγ/IL-17 **(not shown)**. Of note, PDMP or LacCer treatment did not affect astrocyte viability (Supplementary Figs. 7b,c).

To analyze the relative contribution of B4GALT5 and B4GALT6 on astrocyte activation [17,23,24], we knocked-down down *b4galt5* and *b4galt6* expression using lentivirus-delivered shRNAs (Fig. 3b). The knock-down of *b4galt6* suppressed the up-regulation of *h2-Aa, ccl5* and *cxcl10* expression triggered by LPS/IFNγ activation to a similar extent than PDMP treatment. However, the knock-down of *b4galt5* did not have a significant effect (Fig. 3c), suggesting that B4GALT6 plays a dominant role in astrocyte activation. Of note, PDMP treatment of astrocytes in which B4GALT6 had been knocked down with shRNA did not further suppress *h2-Aa, ccl5* and *cxcl10* expression, suggesting that the effects of PDMP result from the specific inhibition of B4GALT6-dependent LacCer synthesis (Supplementary Fig. 7d).

To determine the relative contribution of B4GALT5 and B4GALT6 on EAE progression we used a lentivirus-based system optimized for astrocyte-specific knock-down *in vivo* [25] (Fig. 3d). In this system, the *gfap* promoter drives the expression of an shRNA of choice and a GFP reporter. Following intra-cerebroventricular (i.c.v.) injection of shRNA-encoding lentivirus during the progressive phase of NOD EAE, the GFP reporter was expressed in GFAP+ astrocytes but not Iba1+ microglia and inflammatory macrophages (Fig. 3e and Supplementary Fig. 7e). Consequently, we detected an astrocyte-specific knock-down of *b4galt6* and *b4galt5* expression (Fig. 3e). The knock down of *b4galt6*, but not of *b4galt5*, decreased CNS LacCer levels during the progressive phase of NOD EAE (Fig. 3f). Moreover, the knock down of *b4galt6*, but not of *b4galt5*, suppressed disease progression in NOD mice (Fig 3g), suggesting that LacCer produced by B4GALT6 acts in an autocrine manner to promote astrocyte activation and EAE progression.

To study the molecular mechanisms mediating the effects of LacCer, we searched the promoters of genes regulated by LacCer in primary astrocytes in culture for specific TF binding sites and detected a significant enrichment ($P<10^{-5}$) in NF-κB and ISRE responsive elements.

LacCer is reported to activate NF-kB in astrocytes [18,26] and we confirmed these observations on astrocytes *in vitro* (Supplementary Fig. 7f). The role of IRF1/ISRE in the regulation of astrocyte activity by LacCer, however, is unknown. We found that LacCer treatment enhanced the translocation of IRF-1 to the nucleus, whereas B4GALT6 inhibition interfered with this process (Fig. 3h). Moreover, we detected the recruitment of NF-κB and IRF-1 to the *nos2* promoter in astrocytes activated with LPS/IFNγ (Fig. 3i). To study the functional role of IRF-1 on the response to LacCer we compared the response of WT and IRF-1 deficient astrocytes to activation with LPS/IFNγ. IRF-1 deficiency abrogated the up-regulation triggered by LacCer of *nos2* and other genes that harbor ISRE biding sites in their promoters (*csf2, ccl2, ccl5, il6* and *tlr2*) (Fig. 3j). Moreover, IRF-1 was co-expressed with CCL-2 and iNOS in GFAP+ astrocytes during progressive NOD EAE (Supplementary Fig. 7g). Hence, LacCer produced by B4GALT6 controls astrocyte activity through NF-κB and IRF-1 dependent pathways.

B4GALT6 regulates ccl2 transcriptional activity in astrocytes

Inflammatory monocytes recruited to the CNS by CCL-2 promote neurodegeneration and disease progression in MS and EAE [19–21,27]. Based on the effects of LacCer on *ccl2* expression and NF-κB and IRF-1 activation in astrocytes, we searched the *ccl2* promoter for responsive elements to these transcription factors and identified potential binding sites (Fig. 4a). In reporter assays we found that IRF-1 and NF-κB (p65) transactivate the *ccl2* promoter (Fig. 4b). Moreover, we detected a significant recruitment of NF-κB and IRF-1 to the *ccl2* promoter in astrocytes activated with LPS/IFNγ (Fig. 4c). This recruitment was arrested by the inhibition of LacCer synthesis with PDMP, and the effects of PDMP could be abrogated by the addition of exogenous LacCer (Fig. 4c). Thus, LacCer produced by B4GALT6 controls *ccl2* expression.

To investigate the relevance of the regulation of *ccl2* expression by B4GALT6-LacCer we analyzed the effect of PDMP administration on inflammatory monocytes recruited to the

CNS during NOD EAE. B4GALT6 inhibition reduced the recruitment of inflammatory monocytes (Fig. 4d), and similar results were also obtained when we analyzed the effects of B4GALT6 knocked-down in astrocytes using lentivirus-delivered shRNAs (Fig. 4e). PDMP or LacCer did not affect the viability of purified Ly6C^{high} monocytes, their migration in a CCL-2 gradient, or their response to LPS/IFNγ stimulation (Figs. 4f–i). Thus, B4GALT6 in astrocytes controls CCL-2 production and the recruitment of inflammatory monocytes into the CNS.

B4GALT6 in astrocytes regulates the activation of microglia and CNS-infiltrating monocytes

Microglia play a central role during CNS inflammation [28]. To study the effects of B4GALT5/6 on microglia we analyzed their transcriptional profile by NanoString nCounter in naïve mice, or during the progressive phase of NOD EAE in vehicle- or PDMP-treated mice. We found that B4GALT5/6 inhibition reduced the expression of genes associated with microglia activation during EAE (Figs. 5a,b). Moreover, B4GALT5/6 inhibition led to the down regulation of genes linked to a pro-inflammatory phenotype (M1), concomitant with an up-regulation of anti-inflammatory (M2) associated genes in microglia and CNS-infiltrating monocytes (Figs. 5c and Supplementary Table 3). Thus, although B4GALT5/6 are not up-regulated by microglia during EAE, LacCer modulates the activation of microglia and CNS-infiltrating monocytes.

Given that B4GALT5/6 inhibition *in vivo* altered the M1/M2 balance in microglia and CNS-infiltrating monocytes (Fig. 5c), we studied whether this effect was cell autonomous. We found that neither the viability nor the response of primary mouse microglia to LPS/IFNγ were affected by B4GALT5/6 inhibition or the addition of LacCer in the absence of astrocytes (Figs. 5d–e and Supplementary Figs. 8a,b). LacCer also did not affect the transcriptional response to activation of leptomeningeal phagocytes or choroid plexus cells (Supplementary Figs. 8c,d).

We detected, however, significant effects of PDMP and LacCer on microglial activation in mixed glia cultures containing both microglia and astrocytes (Fig. 5f). To identify the mechanisms involved in the regulation of microglial activation (as indicated by *nos2* up-regulation) by B4GALT6/LacCer in astrocytes we used blocking antibodies. We found that GM-CSF blockade inhibited the LacCer-dependent boost in microglial *nos2* up-regulation (Fig. 5g). Moreover, the B4GALT6/LacCer pathway controlled NF-κB and IRF-1 recruitment to the *csf2* (GM-CSF) promoter during astrocyte activation (Figs. 5h).

To evaluate the physiological relevance of these findings we analyzed *csf2* expression in astrocytes following *b4galt6* knock-down with shRNAs during the chronic phase of NOD EAE. In agreement with our *in vitro* results *b4galt6* knock down resulted in decreased *csf2* expression in astrocytes (Figs. 5i) concomitant with decreased *nos2* expression in microglia (Figs. 5j). Taken together, these data suggest that GM-CSF produced by astrocytes in a B4GALT6/LacCer-dependent manner modulates microglia activation.

B4GALT6 and LacCer levels are up-regulated in MS lesions

To examine the clinical relevance of our findings, we analyzed *B4GALT6* and *B4GALT5* expression in brain samples from MS patients and controls. We found increased expression of *B4GALT5* (2.15±0.28 fold) and *B4GALT6* (8.26±2.11 fold) in MS lesions, but not in normal appearing white matter (NAWM) or controls (Fig. 6a). B4GALT6 co-expression with CCL-2 and iNOS was also detected in GFAP[+] astrocytes from MS patients (Fig. 6b). The increased expression of *B4GALT5/6* was linked to increased LacCer levels in MS lesions (Fig. 6c), suggesting that increased B4GALT6 activity and LacCer levels are also linked to MS pathology.

We next studied whether B4GALT6 modulates the activity of primary astrocytes activated with the TLR-3 agonist poly(I:C) or IL-1β. We found that B4GALT6 inhibition led to a significant decrease in CCL2, *CCL5, COX2, IL6, NOS2* and *TLR2* expression (Fig. 6d). Thus, these results suggest that B4GALT6 is a potential therapeutic target for the regulation of astrocyte activity in human neuroinflammatory disorders.

Discussion

GFAP[high] reactive astrocytes modulate leukocyte infiltration [7,8] and regulate the inflammatory response [5–9] in response to CNS trauma and acute EAE, but their regulation and function during chronic CNS inflammation is poorly understood. We found that B4GALT6 in astrocytes boosts CNS inflammation and promote neurodegeneration during chronic CNS inflammation. B4GALT5 and B4GALT6 are the only two members of the 4-galactosyltransferase family that catalyze LacCer synthesis [17]. Both enzymes are up-regulated by astrocytes during chronic EAE and MS but B4GALT6, and not B4GALT5, is responsible for the increased CNS LacCer levels, astrocyte activation and disease progression. These findings are in line with previous studies that described different biological roles for B4GALT5 and B4GALT6, for example in embryonic development [23,24]. Moreover, Tokuda and coworkers have recently demonstrated that B4GALT6 deficiency results in a significant decrease in LacCer synthase activity in the CNS of naïve mice; LacCer synthesis in the kidney, however, is controlled by B4GALT5 [24]. Taken together, these data suggest a spatial and functional compartmentalization of B4GALT5 and B4GALT6 LacCer synthase activities.

Pro-inflammatory microglia and CNS-infiltrating monocytes, recruited and activated in response to factors present in the inflamed CNS microenvironment, are thought to contribute to the pathogenesis of MS and other neurodegenerative disorders [29–31]. We found that the LacCer synthesized by B4GALT6 in astrocytes controls the production of chemokines and cytokines that regulate inflammatory monocyte and microglia recruitment and activation, such as CCL-2 [19–21,27] and GM-CSF [32]. The effects of LacCer on astrocytes involved IRF-1 and NF-κB, but although LacCer is reported to modulate PKC/cPLA2 signaling [33,34] and membrane microdomains [17], the mechanisms by which LacCer controls these transcription factors are not completely understood.

Lipids exert significant effects on inflammation during autoimmunity and microbial infections, acting either as targets or regulators of the immune response [14,35–40]. Although

lipid-specific antibodies and T cells have been identified in MS [37,39], the role of bioactive lipids in CNS autoimmunity is mostly unknown. Steinman and coworkers recently reported that myelin sheath lipids induce apoptosis in autoreactive T cells and ameliorate EAE [35]. Considering the pro-inflammatory effects of LacCer, it appears that perturbations in the balance of anti- and pro-inflammatory lipids in the CNS play a significant role in MS pathology. Thus, the comprehensive profiling of CNS lipids is likely to identify new targets for therapeutic intervention in MS and also for other neurologic disorders in which astrocyte activation contributes to disease pathology.

In conclusion, our results demonstrate that the LacCer/B4GALT6 axis in astrocytes controls processes that drive CNS inflammation and neurodegeneration. Thus, the modulation of glycolipid synthesis is a potential therapeutic approach for MS and also for other neurologic disorders in which astrocyte activation contributes to disease pathology.

Materials and Methods

Animals

C57BL/6J, NOD/ShiLtJ (NOD), IRF-1 deficient mice and GFAP-HSV-TK mice, were from The Jackson Laboratory. Heterozygote GFAP-HSV-TK bearing C57Bl/6 mice were used to generate F1 littermates that were either GFAP^{TK} or WT F1. Tg(GFP-hGFAP) FVB transgenic mice have been described[41]. All animals were kept in a pathogen-free facility at the Harvard Institutes of Medicine. All experiments were carried out in accordance with guidelines prescribed by the Institutional Animal Care and Use Committee of Harvard Medical School.

EAE induction and treatments

EAE was induced by immunization female mice with MOG$_{35-55}$ peptide emulsified in CFA (Difco Laboratories) at a dose of 100μg (C57BL/6 and F1 mice) or 150μg (NOD mice) per mouse, followed by the administration of pertussis toxin (150 ng per mouse; List biological laboratories, Inc.) on days 0 and 2 as described[14]. Clinical signs of EAE were assessed according to the following score: 0, no signs of disease; 1, loss of tone in the tail; 2, hind limb paresis; 3, hind limb paralysis; 4, tetraplegia; 5, moribund.GCV (APP Pharmaceuticals), or vehicle control (PBS) was administered daily (25mg/kg, subcutaneously) 7 days before EAE induction and continued for the duration of the acute phase (day 15), or only during the progressive/chronic phase (day 30–50). LacCer (Matreya LLC) or vehicle (10% DMSO), were administered at a dose of 10μg per mouse together with the MOG$_{35-55}$ peptide to C57BL/6J mice during EAE induction, and also intraperitoneally (i.p.) every other 3 days henceforth. LacCer or vehicle administration to NOD mice were initiated 35 days after disease induction at a dose of 10μg per mouse given i.p. every 3 other days. PDMP (Matreya LLC) or vehicle control (5% tween-80), were administered at day 40 after EAE induction twice a day with 20mg/kg given i.p. for the duration of the experiment.

Immunofluorescence (IF)

Animals were perfused with 4% paraformaldehyde in 0.1 M PBS. Tissues were cryoprotected in 0.1 M PBS plus 30% sucrose, and cut with cryostat into 10-μm-thick sections. Sections were blocked in 5% goat serum, M.O.M.™ Mouse Ig Blocking reagent (Vector laboratories) containing 0.3% Triton™ X-100 (Sigma-Aldrich), and incubated overnight at 4°C with following antibodies : GFAP (chicken, 1:500, Abcam), GFP (chicken, 1:500, Abcam), IBA-1 (Rabbit, 1:200, Dako), B4GALT6 (Rabbit, 1:100, proteintech), iNOS [mouse (4E5) , 1:100, iNOS], CCL2 [mouse (2D8), 1:100, Fisher scientific], Nestin [mouse (rat-401), Millipore], CD31 [mouse (RM0032-1D12) , 1:100, Abcam], and IRF-1 (rabbit, 1:250, Santa cruz). The next day sections were washed 3 times, and incubated with an appropriate fluorophore-conjugated goat secondary Abs (1:1000; Abcam) for 1 h at room temperature. Six animals/group were used. Images were taken using a LSM 710 confocal microscope (Carl Zeiss).

Isolation of cells from adult mice CNS

Mononuclear cells were isolated from the CNS as previously described [42] with minor modifications. Naïve and EAE mice were euthanatized, and then subjected to perfusion through the left ventricle with ice-cold sterile PBS. Brains and spinal cord were then removed, minced and enzymatically dissociated with 0.05% (w/v) collagenase type III (Worthington Biochemical), 0.5% Dispase II (Roche Applied Science), 40 μg/ml DNAse I, 20 mM HEPES in HBSS) for 30 min at 37C to make a suspension of single cells. Enzymes were inactivated with 20 ml of Ca^{2+}/Mg^{2+}-free HBSS containing 2 mM EDTA and 20 mM HEPES. The digested tissue was triturated and passed through a 100-μM cell strainer. Cells were centrifuged and resuspended in 30% isotonic Percoll (GE Healthcare) and 40 μg/ml DNAse I, underlined by 70% isotonic Percoll, and centrifuged at $1000 \times g$ at 4°C for 25 min. Cells were collected from the 70%−30% interphase, and sorted by FACS Aria.

FACS sorting of astrocytes, microglia and monocytes

These purification procedures are based on previously described dissociation and purification protocols[42,43]. Isolated CNS cells, were incubated with anti-Mouse CD16/CD32 for 15 min on ice to block the Fc receptors, and stained with fluorochrome-conjugated antibody for CD11b (M1/70), CD45(90), CD3 (145-2C11), CD4 (GK1.5), and Ly6C (HK1.4), and Biotion-conjugated GSL I – isolectin B4 (Vector labs), CD105 (N418), CD140a (APA5), CD11c (N418), F4/80 (BM8), O4 (O4, Miltenyi Biotec), and CD19 (eBio1D3), and un-conjugated antibodies recognizing mouse MOG (8–18C5, Millipore), O1 (O1) , and Galactocerebroside (mGlaC, Millipore). All antibodies were from Ebioscience, unless otherwise mentioned (clone number, when relevant, in parentheses). Cells were washed and incubated PE- conjugated Streptavidin and R-Phycoerythrin AffiniPure F(ab')2 fragment of Goat Anti-Mouse IgG + IgM (H+L) (Jackson ImmunoResearch laboratories) for 20 min at 4 C in the dark. Cells were washed, incubated with 7-AAD or Fixable Viability Dye eFluor® 450 (if cells were to be used for intracellular staining), for exclusion of dead cells (Fig. S3A), and sorted as following. Microglia were sorted as CD11b+ cells with low CD45 expression and low Ly6C (CD11b+/CD45^{low}/Ly6C^{low}), while the inflammatory monocytes were considered as CD11b+/Ly6C^{high} [44]. T-cells were sorted as CD3+CD4+

cells. Astrocytes were isolated following the depletion of lymphocytes, microglia, monocytes (Fig. S3B), and oligodendrocytes, and lymphocytes (T-cells, B-cells, and NK cells) (Fig. S3C). Sorted cells were found to be >85% GFAP[+] by FACS analysis (Fig. S3D). We confirmed that we had isolated a relatively pure populations of astrocytes by qPCR for the astrocyte markers[43,45] *gfap, aldh1l1* and *aqp4*, and found them to be exclusively expressed in the astrocyte fraction (in a similar expression pattern to that of GFP[+] astrocytes sorted from Tg(GFP-hGFAP) FVB transgenic mice[41]) (Fig. S3E). We used an additional cohort of markers to explore for presence of immune cells [microglia/monocytes cells – *itgam* (CD11b), *and emr1* (F4/80), dendritic cells - *itgax* (CD11c), NK cells - *Klrb1c* (Nk1.1) , T-cells - *cd3*, and B-cells - *cd19*], oligodendrocytes (*mog, mbp*), and neurons (*syt1, snap25*) (Fig. S3F, G).

LacCer measurement

Chemical standards of LacCer (d18:1/16:0) and LacCer (d18:1/18:0) were obtained from Avanti Polar Lipids. Quantification of LacCer (d18:1/16:0) and LacCer (d18:1/18:0) was achieved by LC-MS/MS analysis performed on an Agilent (Agilent Technologies, Santa Clara, CA) 6460 triple-quadrupole LC/MS/MS system. The fragments from the [M+H][+] ions for LacCer and internal standard were subjected to collision induced dissociation and the two major types of fragment ions were monitored via electrospray ionization in the positive ion mode in multiple reaction monitoring (MRM) mode for each ion. These two MRM transitions corresponded to the loss of the neutral lactosyl moiety, and to the formation of the lactose ion. Specifically, the MRM transitions used for quantification for LacCer (d18:1/16:0) and LacCer(d18:1/18:0) were 862.5>464.5 and 890.6>548.5, respectively. Secondary confirmatory MRM transitions for LacCer(d18:1/16:0) and LacCer(d18:1/18:0) of 862.5>264.3 and 890.6>264.3 were also monitored. Mass spectrometer parameter settings were gas temp (325 °C), gas flow (12 L/min), nebulizer (25 psi), sheath gas temp (400 °C), sheath gas flow (12 L/min), capillary voltage (4000v), and nozzle voltage (500v). Liquid chromatography conditions with an a Phenomenex Gemini C18 column 4.6 × 50 mm 5 μm particle size was used for separation. Chromatography method the following flow rate = 0.4 mLs/min; solvent A = 5mM ammonium formate in 5% MeOH and 0.1%formic acid v/v/v; solvent B = 80% 2-propanol, 15% methanol, 5% water and 0.1% formic acid (v/v/v/v). The gradient started at 20%A and progressed to 100% A in 10 minutes and maintained for the next 10 minutes. The column was re-equilibrated to starting conditions for 5 minutes before the next injection. An internal standard of non-native LacCer (18:1/12:0) was utilized since a stable isotope version was not available. Standard curve mixture was analyzed at various concentrations between 0.10 nM to 3.3 μM in LacCer (d18:1/16:0) and an internal standard concentration of 1 μM. The lower limit of quantification was estimated at 1 nM and a R^2 of 0.9969 was obtained using linear regression analysis. A standard curve with the internal standard doped in was run between 1 nM to 3.3 μM. Since the standards were only available only for LacCer (18:1/16:0), the values for LacCer (18:1/18:0) assumes that the relative ionization efficiency for the two closely related lipids is identical.

Extraction of Lipids

The brain tissue was weighed and homogenized using a Dounce homogenizer (VWR), in the extraction solvent using a Bligh and Dyer type liquid-liquid extraction. All solvents were obtained from Sigma-Aldrich in ultra-high purity. The internal standard LacCer (18:1/12:0) was dissolved in 2:1 chloroform-methanol v/v. 6 ml of 2:1 chloroform-methanol and 2 ml of PBS. After approximately 2 minutes of homogenization, the liquid was transferred to a 8 ml glass vial. The mixture was spun in a high speed centrifuge at 1000g for 20 minutes. This resulted in the formation of a protein disk and insoluble materials in the middle. The bottom layer was removed using a glass Pasteur pipet and transferred to a clean vial for evaporation under a stream of gentle nitrogen. The dried sample was reconstituted in 100 μl of 2:1 chloroform-methanol, and analyzed using the HPLC-MS.

nCounter Gene expression

100 – 200ng of total RNA was hybridized with reporter and capture probes for nCounter Gene Expression code sets (Mouse Inflammation Kit, or a custom made astrocyte-oriented probe set (Table S1)), according to manufacturer's instructions (NanoString Technologies). Data were normalized to spiked positive controls and housekeeping genes (nSolver Analysis system). Transcript counts less than the mean of the negative control transcripts plus 2 standard deviations for each sample were considered background.

Analysis of gene expression data

Nanostring generated gene expression data were analyzed by use of the Expander 6.06 platform [46]. Genes were clustered using the unbiased CLICK algorithm , and each cluster was further analyzed for enrichments in transcription factors binding sites (promoter analysis).

q PCR

RNA was extracted with RNAeasy columns (Qiagen), or TRIzol® (Invitrogen), cDNA was prepared and used for qPCR and the results were normalized to *gapdh* (mice) or *ACTIN* (human). All primers and probes were from Applied Biosystems. *Aldh1l1* (Mm03048957_m1), *aqp4* (Mm00802131_m1), *b4galt5* (Mm00480147_m1), *b4galt6* (Mm00480045_m1), *ccl5* (Mm01302427_m1), *cd19* (Mm00515420_m1), *cd3e* (Mm00599684_g1), *cd40* (Mm00441891_m1), *csf2* (Mm01290062_m1), *cxcl10* (Mm00445235_m1), *emr1* (Mm00802529_m1), *foxp3* (Mm00475162_m1), *gapdh* (Mm00484668_m1), *gfap* (Mm01253033_m1), *h2-Aa* (Mm00439211_m1), *Ifng* (Mm01168134_m1), *Il10* (Mm00439614_m1), *il17a* (Mm00439618_m1), *il1b* (Mm00434228_m1), *il6* (Mm00446190_m1), *irf1* (Mm01288580_m1), *itgam* (Mm00434455_m1), *itgax* (Mm00498698_m1), *klrb1c* (Mm00824341_m1), *mbp* (Mm01266402_m1), *mog* (Mm00447824_m1), *nos2* (Mm00440502_m1), *relb* (Mm00485664_m1), *snap25* (Mm00456921_m1), *spp1* (Mm00436767_m1), *syt1* (Mm00436858_m1), *tbx21* (Mm00450960_m1), *tgfb1* (Mm01178820_m1), *tlr2* (Mm00442346_m1), *tnf* (Mm00443260_g1), *vim* (Mm01333430_m1), *ACTB* (Hs01872448_s1), *B4GALT5* (Hs00941041_m1), *B4GALT6* (Hs00153133_m1), *CCL2*

(Hs01060665_g1), *CCL5* (Hs00941041_m1), *IL6* (Hs00234140_m1), *NOS2* (Hs00174575_m1), *PTGST2* (Hs00191135_m1), and *TLR2* (Hs00985639_m1).

T-cell proliferation and cytokine measurement

Splenocytes and lymph node cells were cultured in X-VIVO medium and were plated for 72h at a density of 5×10^5 cells per well in the presence of MOG_{35-55} peptide. During the final 16h, cells were pulsed with 1 Ci [3H]thymidine (PerkinElmer), followed by collection on glass fiber filters and analysis of incorporated [3H]thymidine in a -counter (1450 MicroBeta TriLux; PerkinElmer). Supernatants were collect after 48 h of culture for cytokine measurement by enzyme-linked immunosorbent assay [14]. For intracellular cytokine staining, cells were stimulated for 6 h with PMA (phorbol 12-myristate 13-acetate; 50 ng/ml; Sigma), ionomycin (1 μg/ml; Sigma) and monensin (GolgiStop; 1 ml/ml; BD Biosciences). After staining of surface markers, cells were fixed and made permeable according to the manufacturer's instructions BD Cytofix/Cytoperm™ Kit (BD Biosciences), or Foxp3 Fixation/Permeabilization (Ebiosceince).

Mouse primary microglia

Mouse primary microglia were prepared as described [47] with minor modifications. Cerebral cortices from 1- to 3-day-old neonatal mice were dissected, carefully stripped of their meninges, digested with 0.25% trypsin, and dispersed into a single-cell level. The cell suspension ("mixed glia") was then cultured at 37°C in humidified 5% CO2–95% air. Medium was replaced every 4–5 days. Mixed glia cultures reached confluence after 7–10 days, and were used to harvest microglia between 15 and 20 days after preparation. Microglia were isolated by the mild trypsinization procedure (Mild T/E) as previously described[47] . Briefly, treatment of the confluent mixed glial cultures with 0.06% trypsin (mild T/E) resulted in detachment of an intact layer of cells containing almost all the astrocytes and leaving behind a highly enriched population of microglia (>98%, as determined by staining with fluorescein-conjugated Griffonia simplicifolia isolectin B4 (IB4) (Vector Laboratories) or PE-conjugated CD11b Ab (data not shown)). The attached microglia were allowed to recover for 24–48 hours.

Mouse Primary Astrocytes

Mix Glia was prepared as above, and incubated with 20ug/ml biotin anti-IB4 (Vector Labs) for 20 min at RT, washed and incubated with Streptavidin – conjugated magnetic beads (Miltenyi Biotec) for 15 min at 4C. Cells were washed, and cleared of IB4+ cells (microglial and endothelial cells)[43] using cell separation Columns (Miltenyi Biotec). Cells were then cultured until confluent (day 7–10), the astrocyte monolayer was separated using the mild trypsinization procedure, separated into single cells suspension with Accutase (Invitrogen) and plated. Cells were >98% astrocytes, as determined by staining with GFAP or GLAST, with less than 2% contamination of CD11b+ microglia cells (data not shown)).

Mouse primary leptomeningeal phagocytes

The meninges were carefully stripped from the brains of 1- to 3-day-old neonatal mice, and digested with 1% collagenase for 20 min at 37°C, and then dispersed into a single-cell level.

Isolated cells, were incubated with anti-mouse CD16/CD32 for 15 min on ice to block the Fc receptors, and stained with APC-conjugated antibody for CD11b (M1/70) for 30 min at 4°C. Cells were washed, incubated with 7-AAD for exclusion of dead cells, and sorted.

Mouse Primary choroid plexus cells

Mouse primary choroid plexus cells were prepared as described[48,49] with minor modifications. In brief, the choroid plexus was removed from 1- to 3-day-old neonatal mice, digested with 1% collagenase for 20min at 37°C, and then dispersed into a single-cell level. The cell suspension was washed in culture medium for choroid plexus cells [Dulbecco's modified Eagle medium/ Ham's F12 (Invitrogen) supplemented with 10% foetal calf serum (Sigma-Aldrich), 1 mM l-glutamine, 1 mM sodium pyruvate, 100 U/ ml penicillin, 100mg/ml streptomycin, 5mg/ml insulin, 20mM Ara-C) and cultured (2.5×10^5 cells/well) at 37°C, 5% CO2 in poly-D-lysine coated 24-well plates. After 24h, the medium was changed, and the cells were either left untreated or treated as described.

Plasmids

The dual reporter construct expressing Gaussia luciferase under the murine *Ccl2* promoter, and Secreted alkaline phosphatase (SEAP) under the CMV promoter (used for transfection normalization), was from GeneCopoeia, Inc. The construct encoding IRF1 was from Addgene. The pLenti-GFAP-EGFP-mir30-shAct1 vector [25] was a kind gift from Dr. Guang-Xian Zhang (Thomas Jefferson University, PA, USA).

In vitro knock-down with shRNA

The expression of LacCer synthases was knocked-down in C8-D30 astrocytes, using shRNA lentiviruses particles against *b4galt5* (TRCN0000018782), *b4galt6* (TRCN0000334278), or a non-targeting sequence (TRCN0000018782) as a control (Sigma). Astrocytes were incubated with lentiviruses and 8 μg/ml polybrene (both from Sigma-Aldrich) for 12 h, allowed to recover for 24h, and were selected with puromycin (2 μg/ml). Gene knock-down in puromycin-resistant cells was verified by qPCR.

In vivo astrocyte-specific knock-down with shRNA Lentivirus

pLenti-GFAP-EGFP-mir30-shRNA harboring shRNA sequences against *b4galt5, b4galt6*, and a non-targeting shRNA were cloned using the pLenti-GFAP-EGFP-mir30-shAct1 vector [25] as a backbone, by replacing the shRNA for Act1 with the above-mentioned *in vitro* validated shRNA sequences (*b4galt5* : 5' - GCAGCCTGAATGACTCAGATT*ctcgag*AATCTGAGTCATTCAGGCTGC-3', *b4galt6* : 5'-CGATGGACTGAACAATTTATT*ctcgag*AATAAATTGTTCAGTCCACG-3', and a non-targeting shRNA : 5'- GCGCGATAGCGCTAATAATTT*ctcgag*AAATTATTAGCGCTA-TCGCGC-3'). Lentivirus particles were then generated by transfecting 293FT cells (Invitrogen) with 3 μg of the newly generated pLenti-GFAP-EGFP-mir30-shRNA vectors and 9 μg of the ViraPower™ Packaging mix (The helper plasmids pLP1, pLP2, pLP/VSV-G, Invitrogen). 48h later supernatants were collected, filtered through a 0.45μM PVDF filter, and concentrated overnight with the Lenti-X™ concentrator kit (Clontech) according to the

manufacture's instructions. The viral titrate was determined using the Lenti-X™ qRT-PCR titration kit (Clontech) according to the manufacture's instructions, and stored at −70°C.

For *in vivo* injection, NOD EAE mice, 35 days after immunization (progressive phase) were anesthetized by an i.p. injection of ketamine (100 mg/kg) and xylazine (20 mg/kg) and placed in a Kopf Stereotaxic Alignment System. Using a Hamilton syringe, 1×10^7 IU/mouse of shB4galt5, shBrgalt5, shControl (non-targeting) virus were injected 0.44 mm posterior to the bregma, 1.0 mm lateral to it and 2.2 mm below the skull surface. Injection speed was maintained at 1 μl/minute to prevent leaking.

Viability Assay

Astrocytes, microglia or Ly6Chigh monocytes were pre-treated with indicited concentrations of PDMP or LaCcer, and further activated with LPS/IFNγ (microglia and astrocytes), CCL-2 (monocytes), or left untreated. Viability was assed following activation using the CellTiter-Fluor™ Cell viability assay (Promega).

Subcellular fractionation and Immunoblot analysis

Astrocytes were treated as indicated, and total extracts (30μg of protein), or the nuclear and cytoplasmic subcellular fractionations of cells, were separated by NuPAGE 10% Bis-Tris Gel (Invitrogen), and electroblotted onto supported nitrocellulose membrane. Subcellular fractionations were prepared using the NE-PER® Nuclear and Cytoplasmic Extraction kit (Pierce Biotechnology), according the manufacture instruction. Blot were probed with Rabbit anti-IRF-1 (D5E4) XP® Rabbit mAb, GAPDH (D16H11) XP® Rabbit mAb, Lamin B1 polyclonal Rabbit Abs, NF-κB p65 (D14E12) XP® Rabbit mAb, followed by goat anti-rabbit IgG peroxidase conjugate Abs (all antibodies from Cell signaling). The blots were developed using the SuperSignal West Pico chemiluminescence kit (Pierce Biotechnology). Each blot was reprobed with GAPDH (total extract, or cytoplasmic fractionation) or Lamin B1 (nuclear fractionation) to verify protein uniformity. Data quantification was done using Image Studio software (Version 3.1.4) (LI-COR, Inc.)

Transfection and luciferase assay

293T cells were grown in DMEM supplemented with 10% FBS, transfected with Fughene-HD Transfection Reagent (Roche) with the CCL2 dual-reporter and constructs encoding IRF1, NF-κB p65, or an appropriate empty control. Luciferase and SEAP activity was analyzed 24 h after transfection with the Secrete-Pair Dual Luminescence Assay Kit (GeneCopoeia, Inc).

ChIP

Cells were crosslinked with 1% formaldehyde for 15 min. Crosslinking was stopped by the addition of Glycine, and cells were lysed with 0.35 ml lysis buffer (1% SDS, 10 mM EDTA and 50 mM Tris-HCl, pH 8.1) containing 1× protease inhibitor 'cocktail' (Roche Molecular Biochemicals). Chromatin was sheared by sonication and supernatants were collected after centrifugation and diluted in buffer (1% Triton X-100, 2 mM EDTA, 150 mM NaCl nd 20 mM Tris-HCl, pH 8.1). Antibody (5 μg) was prebound for 6 h to protein A and protein G Dynal magnetic beads (Invitrogen) and was washed three times with ice-cold 5% BSA in

PBS, and then was added to the diluted chromatin and immunoprecipitated overnight (antibodies described below). Magnetic bead–chromatin complexes were then washed three times in RIPA buffer (50 mM HEPES, pH 7.6, 1 mM EDTA, 0.7% sodium deoxycholate, 1% Nonidet-P40 and 0.5 M LiCl), followed by three times with Tris-EDTA buffer. Immunoprecipitated chromatin was then extracted with 1% SDS, 0.1 M NaHCO3 and heated for at least 8 h at 65 °C for reversal of the formaldehyde crosslinking. DNA fragments were purified with a QIAquick DNA purification Kit (Qiagen) and analyzed by SYBR Green real-time PCR (primers described below). The following antibodies were used for ChIP: anti-IRF1 (SC-640x; Santa Cruz Biotechnology), anti-NF-κB p65 (ab7970; Abcam), and rabbit IgG (ab27478; Abcam). The following primer pairs were used: The following primer pairs were used: *ccl2*:NF-κB forward, 5′-CAGCTAAATATCTCTCCCGAAGG-3′, and reverse, 5′-CATAGATGCCCACAGCTCAT-3′; *ccl2*: ISRE forward, 5′-CTGCCAATTCTTCCCTCTTTC-3′, and reverse, 5′-GTGGGTTGGA-ATTTGGTATTT-3′; *csf2*: NF-κB forward, 5′- GACCAGATGGGTGGAGTGACC-3′, and reverse, 5′-AGCCACACGCTTCTGGTTCC-3′; *csf2:ISRE* forward, 5′- GCTTTCGAGGGTCA-GATAACA-3′, and reverse, 5′- CACACGCTTGGGCTAAGA-3′; *nos2*:NF-κB(1) forward, 5′-CACAGACTAGGAGTGTCCATCA-3′, and reverse, 5′-GCAGCAGCCATCAGGTATTT-3′; *nos2*:ISRE/NF-κB(2) forward, 5′-ACCATGCGAAGATGAGTGGA-3′, and reverse, 5′- AGCC-AGGAACACTACACAGAA-3′.

Monocytes migration assay

Splenic Ly6C^{high} monocytes were sorted (CD11b⁺/F4–80⁺, SSC^{low}/Ly6C^{high}), and seeded in the upper chamber of a 24-well cell culture insert with 3-μm pore-size (Corning). Cells were pre-treated with PDMP, LacCer, PDMP+LacCer or vehicle for 1h. Then inserts were transferred to different wells with pre-warmed media containing CLL-2 (50 ng/ml, peprotech) or vehicle (PBS). Migrating monocytes were quantified in the lower chamber after 3 hr.

Human primary astrocytes

Human fetal astrocytes were isolated as previously described[50] from human CNS tissue from fetuses at 17–23 wk of gestation obtained from the Human Fetal Tissue Repository (Albert Einstein College of Medicine, Bronx, NY) following Canadian Institutes for Health Research-approved guidelines. Cultures were >90% pure.

MS tissues

Brain tissue was obtained from MS patients with clinically diagnosed and neuropathologically confirmed MS, non-MS CNS inflammatory diseases (NMSCID, including viral encephalitis, Rasmussen's encephalitis and ADEM and healthy controls. Autopsy samples were immediately frozen in liquid nitrogen. White matter MS tissue samples were selected as previously described[51]. All patients and controls, or their next of kin, had given informed consent for autopsy and use of their brain tissue for research

purposes. Ethic approval was given prior to autopsy (CHUM ethic approval: SL05.022 and SL05.023 and BH07.001).

Statistical analysis

Prism software version 6.0e (GraphPad Software) was used for statistical analysis. P values of less than 0.05 were considered significant.

Supplementary Material

Refer to Web version on PubMed Central for supplementary material.

Acknowledgments

References

1. Clarke LE, Barres BA. Emerging roles of astrocytes in neural circuit development. Nat Rev Neurosci. 2013; 14:311–321. [PubMed: 23595014]

2. Rouach N, Koulakoff A, Abudara V, Willecke K, Giaume C. Astroglial metabolic networks sustain hippocampal synaptic transmission. Science. 2008; 322:1551–1555. [PubMed: 19056987]

3. Seifert G, Schilling K, Steinhauser C. Astrocyte dysfunction in neurological disorders: a molecular perspective. Nat Rev Neurosci. 2006; 7:194–206. [PubMed: 16495941]

4. Tsai HH, et al. Regional astrocyte allocation regulates CNS synaptogenesis and repair. Science. 2012; 337:358–362. [PubMed: 22745251]

5. Bush TG, et al. Leukocyte infiltration, neuronal degeneration, and neurite outgrowth after ablation of scar-forming, reactive astrocytes in adult transgenic mice. Neuron. 1999; 23:297–308. [PubMed: 10399936]

6. Myer DJ, Gurkoff GG, Lee SM, Hovda DA, Sofroniew MV. Essential protective roles of reactive astrocytes in traumatic brain injury. Brain. 2006; 129:2761–2772. [PubMed: 16825202]

7. Toft-Hansen H, Fuchtbauer L, Owens T. Inhibition of reactive astrocytosis in established experimental autoimmune encephalomyelitis favors infiltration by myeloid cells over T cells and enhances severity of disease. Glia. 2011; 59:166–176. [PubMed: 21046558]

8. Voskuhl RR, et al. Reactive astrocytes form scar-like perivascular barriers to leukocytes during adaptive immune inflammation of the CNS. J Neurosci. 2009; 29:11511–11522. [PubMed: 19759299]

9. Mayo L, Quintana FJ, Weiner HL. The innate immune system in demyelinating disease. Immunol Rev. 2012; 248:170–187. [PubMed: 22725961]

10. Nylander A, Hafler DA. Multiple sclerosis. J Clin Invest. 2012; 122:1180–1188. [PubMed: 22466660]

11. Weiner HL. The challenge of multiple sclerosis: how do we cure a chronic heterogeneous disease? Ann Neurol. 2009; 65:239–248. [PubMed: 19334069]

12. Joseph J, Bittner S, Kaiser FM, Wiendl H, Kissler S. IL-17 silencing does not protect nonobese diabetic mice from autoimmune diabetes. J Immunol. 2012; 188:216–221. [PubMed: 22116823]

13. Basso AS, et al. Reversal of axonal loss and disability in a mouse model of progressive multiple sclerosis. J Clin Invest. 2008; 118:1532–1543. [PubMed: 18340379]

14. Farez MF, et al. Toll-like receptor 2 and poly(ADP-ribose) polymerase 1 promote central nervous system neuroinflammation in progressive EAE. Nat Immunol. 2009; 10:958–964. [PubMed: 19684606]

15. Cao W, et al. Leukemia inhibitory factor inhibits T helper 17 cell differentiation and confers treatment effects of neural progenitor cell therapy in autoimmune disease. Immunity. 2011; 35:273–284. [PubMed: 21835648]

16. Pluchino S, et al. Injection of adult neurospheres induces recovery in a chronic model of multiple sclerosis. Nature. 2003; 422:688–694. [PubMed: 12700753]

17. Chatterjee S, Alsaeedi N. Lactosylceramide synthase as a therapeutic target to mitigate multiple human diseases in animal models. Adv Exp Med Biol. 2012; 749:153–169. [PubMed: 22695844]

18. Pannu R, Won JS, Khan M, Singh AK, Singh I. A novel role of lactosylceramide in the regulation of lipopolysaccharide/interferon-gamma-mediated inducible nitric oxide synthase gene expression: implications for neuroinflammatory diseases. J Neurosci. 2004; 24:5942–5954. [PubMed: 15229242]

19. Ajami B, Bennett JL, Krieger C, McNagny KM, Rossi FM. Infiltrating monocytes trigger EAE progression, but do not contribute to the resident microglia pool. Nat Neurosci. 2011; 14:1142–1149. [PubMed: 21804537]

20. Izikson L, Klein RS, Charo IF, Weiner HL, Luster AD. Resistance to experimental autoimmune encephalomyelitis in mice lacking the CC chemokine receptor (CCR)2. J Exp Med. 2000; 192:1075–1080. [PubMed: 11015448]

21. Mildner A, et al. CCR2+Ly-6Chi monocytes are crucial for the effector phase of autoimmunity in the central nervous system. Brain. 2009; 132:2487–2500. [PubMed: 19531531]

22. Watkins TA, Emery B, Mulinyawe S, Barres BA. Distinct stages of myelination regulated by gamma-secretase and astrocytes in a rapidly myelinating CNS coculture system. Neuron. 2008; 60:555–569. [PubMed: 19038214]

23. Nishie T, et al. Beta4-galactosyltransferase-5 is a lactosylceramide synthase essential for mouse extra-embryonic development. Glycobiology. 2010; 20:1311–1322. [PubMed: 20574042]

24. Tokuda N, et al. beta4GalT6 is involved in the synthesis of lactosylceramide with less intensity than beta4GalT5. Glycobiology. 2013; 23:1175–1183. [PubMed: 23882130]

25. Yan Y, et al. CNS-specific therapy for ongoing EAE by silencing IL-17 pathway in astrocytes. Molecular therapy : the journal of the American Society of Gene Therapy. 2012; 20:1338–1348. [PubMed: 22434134]

26. Lee JK, et al. Lactosylceramide Mediates the Expression of Adhesion Molecules in TNF-alpha and IFNgamma-stimulated Primary Cultured Astrocytes. The Korean journal of physiology & pharmacology : official journal of the Korean Physiological Society and the Korean Society of Pharmacology. 2011; 15:251–258.

27. Huang DR, Wang J, Kivisakk P, Rollins BJ, Ransohoff RM. Absence of monocyte chemoattractant protein 1 in mice leads to decreased local macrophage recruitment and antigen-specific T helper cell type 1 immune response in experimental autoimmune encephalomyelitis. J Exp Med. 2001; 193:713–726. [PubMed: 11257138]

28. Heppner FL, et al. Experimental autoimmune encephalomyelitis repressed by microglial paralysis. Nat Med. 2005; 11:146–152. [PubMed: 15665833]

29. David S, Kroner A. Repertoire of microglial and macrophage responses after spinal cord injury. Nat Rev Neurosci. 2011; 12:388–399. [PubMed: 21673720]

30. Lawrence T, Natoli G. Transcriptional regulation of macrophage polarization: enabling diversity with identity. Nat Rev Immunol. 2011; 11:750–761. [PubMed: 22025054]

31. Murray PJ, Wynn TA. Protective and pathogenic functions of macrophage subsets. Nat Rev Immunol. 2011; 11:723–737. [PubMed: 21997792]

32. Ponomarev ED, et al. GM-CSF production by autoreactive T cells is required for the activation of microglial cells and the onset of experimental autoimmune encephalomyelitis. J Immunol. 2007; 178:39–48. [PubMed: 17182538]

33. Gong N, Wei H, Chowdhury SH, Chatterjee S. Lactosylceramide recruits PKCalpha/epsilon and phospholipase A2 to stimulate PECAM-1 expression in human monocytes and adhesion to endothelial cells. Proc Natl Acad Sci U S A. 2004; 101:6490–6495. [PubMed: 15084746]

34. Nakamura H, et al. Lactosylceramide interacts with and activates cytosolic phospholipase A2alpha. The Journal of biological chemistry. 2013; 288:23264–23272. [PubMed: 23801329]

35. Ho PP, et al. Identification of naturally occurring fatty acids of the myelin sheath that resolve neuroinflammation. Sci Transl Med. 2012; 4 137ra173.

36. Jahng A, et al. Prevention of autoimmunity by targeting a distinct, noninvariant CD1d–reactive T cell population reactive to sulfatide. J Exp Med. 2004; 199:947–957. [PubMed: 15051763]

37. Kanter JL, et al. Lipid microarrays identify key mediators of autoimmune brain inflammation. Nat Med. 2006; 12:138–143. [PubMed: 16341241]

38. Quintana FJ, et al. Antigen microarrays identify unique serum autoantibody signatures in clinical and pathologic subtypes of multiple sclerosis. Proc Natl Acad Sci U S A. 2008; 105:18889–18894. [PubMed: 19028871]

39. Quintana FJ, Yeste A, Weiner HL, Covacu R. Lipids and lipid-reactive antibodies as biomarkers for multiple sclerosis. J Neuroimmunol. 2012; 248:53–57. [PubMed: 22579051]

40. Schwab JM, Chiang N, Arita M, Serhan CN. Resolvin E1 and protectin D1 activate inflammation-resolution programmes. Nature. 2007; 447:869–874. [PubMed: 17568749]
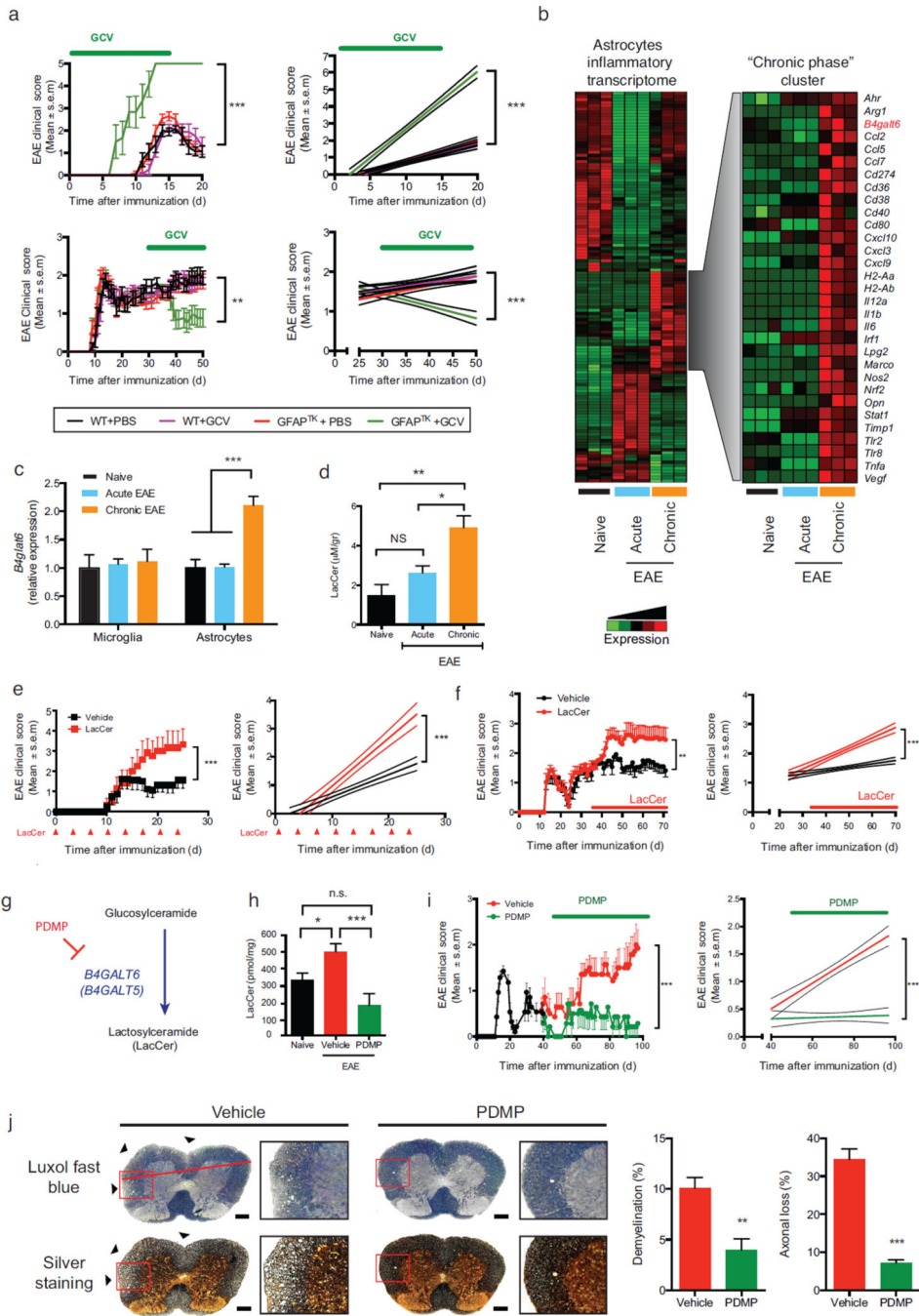
Figure 1. B4GALT6 activity controls CNS inflammation and neurodegeneration

(a) EAE scores in wild type (WT) and GFAP-TK transgenic (GFAP[TK]) F1 hybrid mice (mean and s.e.m.). Right panel, linear-regression curve; dashed lines indicate 95% confidence interval of the regression line. Mice were treated daily with Ganciclovir (GCV, 25mg/kg) or vehicle (PBS) as indicated (green bar). Representative data of three independent experiments with n   7 mice/group. **(a, upper panel)** Mice were pretreated 7 days before EAE induction and continuously until day 15, **(a, lower panel)** or were treated only during the progressive phase (days 30–50). **(b, left panel)** Heatmap depicting the

differential mRNA expression profiles in astrocytes isolated from the CNS of naïve NOD mice, or during the acute or the progressive phase of NOD EAE, as detected by Nanostring nCounter analysis; Representative data of three independent experiments. **(b, right panel)** Heatmap depicting a unique gene cluster specifically up-regulated during the progressive phase of EAE. **(c)** qPCR analysis of *b4galt6* expression in microglia or astrocytes from naïve or EAE NOD mice; expression normalized to *gapdh* and presented relative to that of cells from naïve mice. Representative data of three independent experiments, statistical analysis by Student's t-test. **(d)** Quantification of lactosylceramide (LacCer) in the CNS of naïve or EAE NOD mice, relative to net tissue weight. Representative data of three independent experiments with n 15 samples per condition, statistical analysis by Student's t-test. **(e, f)** EAE clinical scores in C57BL/6 **(e)** and NOD **(f)** mice following administration of LacCer (10μg per mouse) or vehicle as indicated by red arrows or bar. Representative data of two independent experiments with n 8 mice/group. Statistical analysis as in **(a)**. **(e)** EAE scores following LacCer or vehicle administration together with the $MOG_{(35-55)}$ peptide to C57BL/6 mice during EAE induction, and also intraperitoneally (i.p.) every other 3 days henceforth (mean and s.e.m.). **(f)** EAE scores following LacCer or vehicle administration initiated at day 35 after EAE induction (progressive phase). **(g)** PDMP inhibits LacCer synthesis by B4GALT6. **(h)** Quantification of LacCer levels in the CNS of naïve or EAE NOD mice treated with PDMP or vehicle as shown in **(i)**. **(i)** Clinical scores of EAE in NOD mice treated with PDMP or vehicle, administered daily (20mg/kg given i.p. twice a day) from day 40 after EAE induction (progressive phase) for the duration of the experiment Representative data of three independent experiments with n 8 mice/group). **(j)** Histopathology analysis of lumbar spinal cord sections from EAE NOD mice treated with PDMP or vehicle as in **(i)** and stained with Luxol fast blue or Bielschowsky's silver stain for analysis of demyelination or axonal loss, respectively. Scale bar 100 μM. Representative data of two independent experiments with n 6 mice/group (mean and s.e.m.). *P<0.05, **P<0.01, ***P<0.001, n.s. not significant.

Figure 2. B4GALT6 inhibition suppresses astrocyte activation during EAE
(a) Heatmap depicting mRNA expression, as detected by Nanostring nCounter analysis, in astrocytes isolated from naïve or EAE NOD mice treated with PDMP or vehicle (vehicle). Upper panels, histogram presentation of normalized gene expression in each gene cluster. Representative data of three independent experiments, statistical analysis by Student's t-test.
(b) qPCR analysis of *ccl2, ccl5, cxcl10, il1b, nos2, opn, H2-Aa, vim* and *tlr2* expression in astrocytes isolated from naïve and EAE NOD mice treated with vehicle or PDMP; expression is presented relative *gapdh*. Representative data of three independent

experiments, statistical analysis by Student's t-test. (**c**) Relative expression (to NOD naïve group) of genes associated with the control of myelination (Supplementary Table 2) in astrocytes isolated from EAE NOD mice treated with vehicle or PDMP. Representative data of three independent experiments. Statistical analysis by Student's t-test. (**d, e**) qPCR analysis of *Irf1*(**d**) and *Relb*(**e**) expression performed as in (**b**). All data presented as mean and s.e.m. *P < 0.05, **P < 0.01, ***P < 0.001 and n.s. not significant.
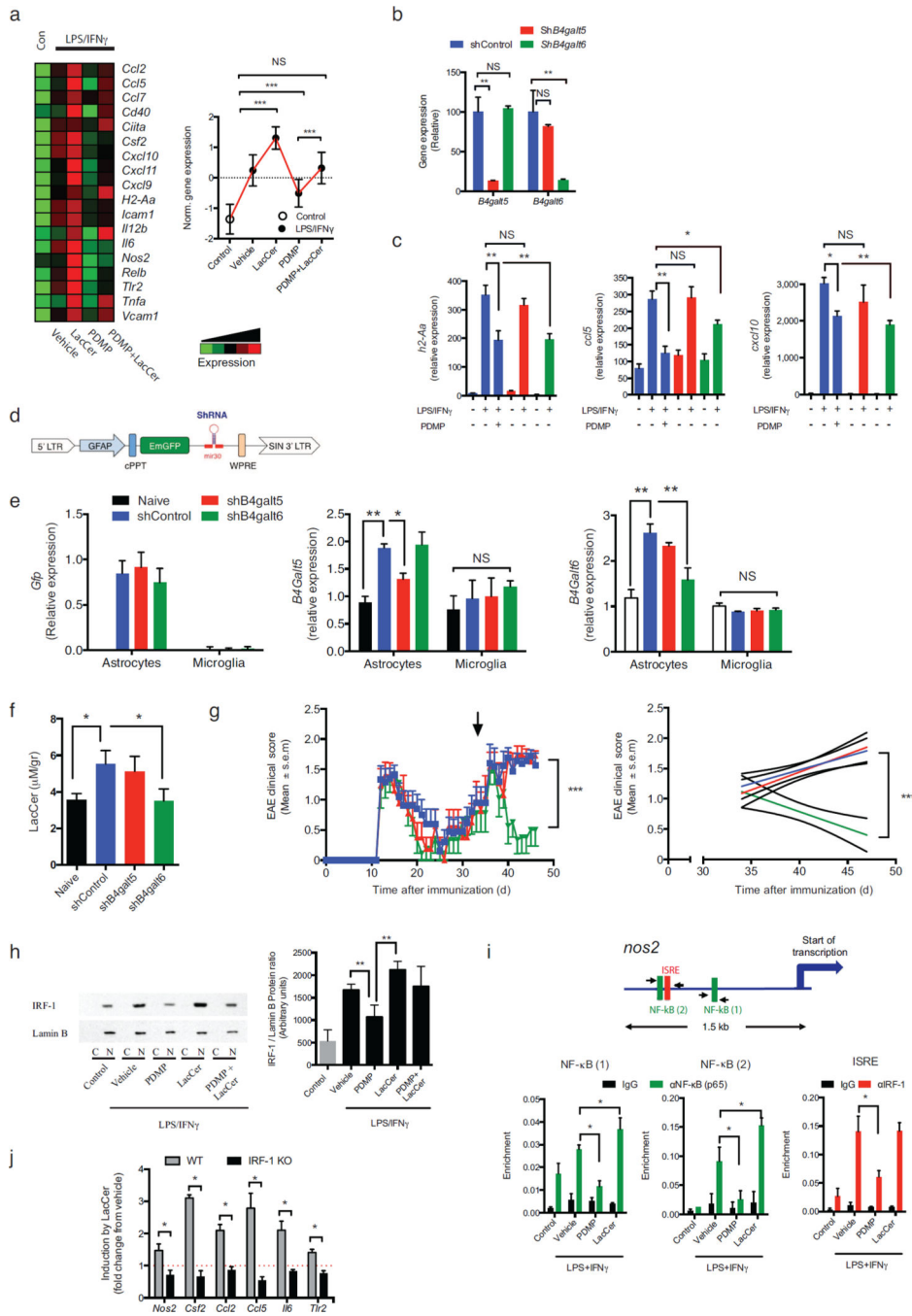
Figure 3. LacCer produced by B4GALT6 acts in an autocrine manner to boost astrocyte activation

Cultured astrocytes were pre-treated for 1h with PDMP (25μM), LacCer (10μM), both (LacCer+PDMP), or vehicle (vehicle), followed by activation with lipopolysaccharide (100 ng/ml) and Interferon-γ (100 Units/ml) (LPS/IFNγ) or left un-treated (control). (**a**) mRNA expression, as detected by Nanostring nCounter analysis, in astrocytes stimulated with LPS/IFNγ, presented as Heatmap (right panel) and histogram presentation of the normalized gene expression (left panel). Representative data of three independent experiments, statistical

analysis by one-way ANOVA followed by Tukey post-hoc analysis. (**b-c**) The expression of *B4galt5 (shB4galt5)*, *B4galt6 (shB4galt6)* or non-targeting shRNA (ShControl) in C8-D30 astrocytes was knocked-down using verified shRNA (n 4). (**b**) qRT analysis of *B4galt5* and *B4galt6* mRNA expression. (**c**) astrocytes were activated as in (**a**) and mRNA expression for *H2-Aa, Ccl5* and *Cxcl10* was determined; expression is presented relative to house keeping gene (*Gapdh*) (n 4). (**d**) Schematic map of the astrocyte-specific shRNA lentiviral vector. (**e–g**) i.c.v. injection of astrocyte-specific shB4galt6 lentivirus ameliorates disease severity. NOD mice were injected i.c.v. with 1×10^7 IU of shControl, shB4galt5 or shB4galt6 lentivirus, at day 35 after EAE induction (progressive phase). n = 10 mice per group (**e, f**) 10 days after i.c.v. injection experiment was terminated and (**e**) *b4galt5* and *b4galt6* expression levels were determined by qPCR in astrocytes isolated from naïve or EAE NOD mice; expression normalized to *gapdh* and presented relative to that of cells from naïve mice. Representative data of two independent experiments, Statistical analysis by one-way ANOVA, followed by Tukey post-hoc analysis. (**f**) LacCer levels were quantified of in the CNS of naïve or EAE NOD mice treated as shown in (**g**). Statistical analysis by one-way ANOVA, followed by Tukey post-hoc analysis. (**g**) EAE clinical scores. Representative data of two independent experiments. Statistical analysis as in (Fig. 1a). (**h**) Cultured primary astrocytes were pre-treated for 1h with PDMP (25μM), LacCer (10μM), both (LacCer +PDMP), or vehicle control (vehicle), followed by activation with LPS/IFNγ for 45min, or left un-treated (control, Con). IRF-1 and Lamin B expression in the nuclear fraction analyzed by western blot and the degree of IRF-1 translocation to the nucleus was assessed by the ratio between the expression of IRF-1 and Lamin-B in the nuclear fractions following densitometric quantification on four independent experiments (right panel). Statistical analysis by one-way ANOVA, followed by Tukey post-hoc analysis. (**i**) ChIP analysis of the interaction of NF- κB, and IRF-1 with the*) nos2* promoter in primary cultured astrocytes. Experimental design and data analysis as in (Fig. 4c). Data from two independent experiments (**j**) qPCR analysis of the expression of *nos2, csf2, ccl2, ccl5, il6*, and *tlr2* in astrocyte cultures established from WT or IRF-1 deficient (IRF-1 KO) mice, pre-treated with LacCer or vehicle, and activated with LPS/IFNγ. Mean gene induction in response to LacCer treatment in LPS/IFNγ-activated cells from 5 independent experiments. Statistical analysis by Student's t-test. All data presented as mean and s.e.m. *P<0.05, **P<0.01, ***P<0.01 and n.s. not significant.
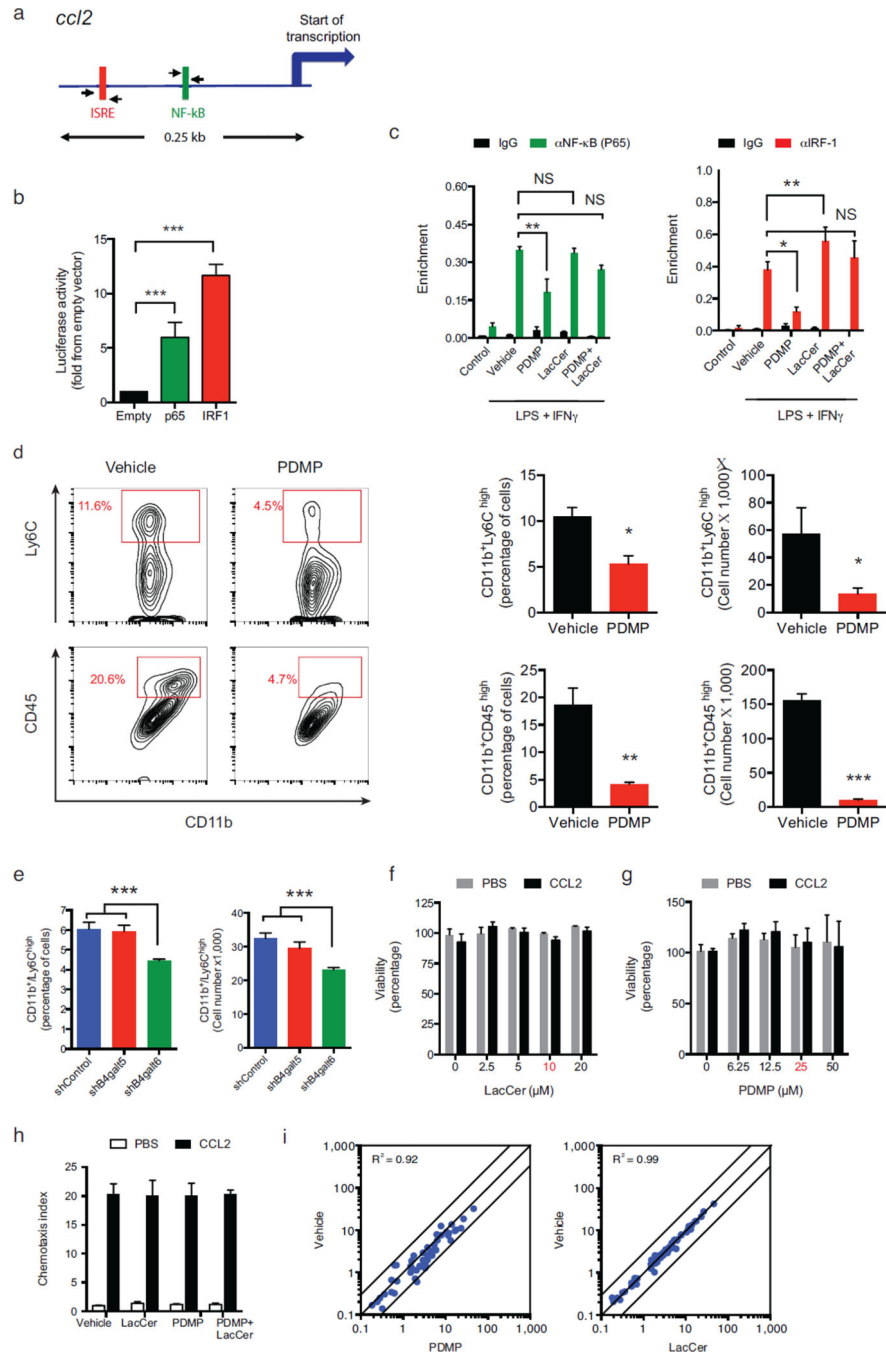
Figure 4. B4GALT6 regulates *ccl2* transcriptional activity in astrocytes
(**a**) Murine *ccl2* promoter. (**b**) Luciferase activity in 293T cells transfected with the *ccl2* luciferase reporter plus one of the following constructs encoding IRF-1, p65 or an empty control vector (Empty). Results are relative to secreted alkaline phosphatase activity, presented as fold induction from empty vector. Data from three independent experiments, statistical analysis by Student's t-test. (**c**) ChIP analysis of the interaction of NF- κB, and IRF-1 with the *ccl2* promoter in primary cultured astrocytes, pre-treated with PDMP and LacCer and activated with LPS/IFNγ (as in Fig. 3), 2 hours following LPS/IFNγ induction.

(**d**) Recruitment of inflammatory monocytes (defined either as of CD11b$^+$ Ly6C^{high} or CD11b$^+$CD45^{high} cells) to the CNS of EAE NOD mice treated with PDMP or vehicle, as in (Fig. 1i), analyzed by flow cytometry and presented as cell frequency, and total cell numbers. Representative data of three independent experiments. Statistical analysis by Student's t-test. (**e**) The frequency and number of CD11b$^+$ Ly6C^{high} monocytes as determined in the CNS 10 days after the i.c.v. injection of astrocytes-specific shRNA lentivirus as in (Fig. 3g) . Representative data of two independent experiments. Statistical analysis by one-way ANOVA, followed by Tukey post-hoc analysis. (**f–h**) monocytes were pre-treated for 1h with PDMP, LacCer, both (LacCer+PDMP), or vehicle, and monocytes chemotaxis was measured using a transwell chamber system. CCL2 or PBS were added to the lower compartment, and 3h later cell viability (**f, g**) and the number of the migrating monocytes (**h**) and cell viability were determined. Migration data is presented as fold from control, and cell viability as percentage from control. Working concentrations are marked in red. Representative data of four independent experiments. (**i**) CD11b$^+$ Ly6C^{high} monocytes were treated with PDMP, LacCer or vehicle, followed by activation with LPS/IFNγ for 6h or left un-treated (control) as in (Fig. 3a). mRNA expression was determined by nCounter Nanostring analysis. Statistical analysis by two ANOVA showed no significance effect of the LacCer or PDMP treatments on the monocytes migration. For all data, data presented as mean and s.e.m. *P<0.05, **P<0.01, ***P<0.001 and n.s. not significant.
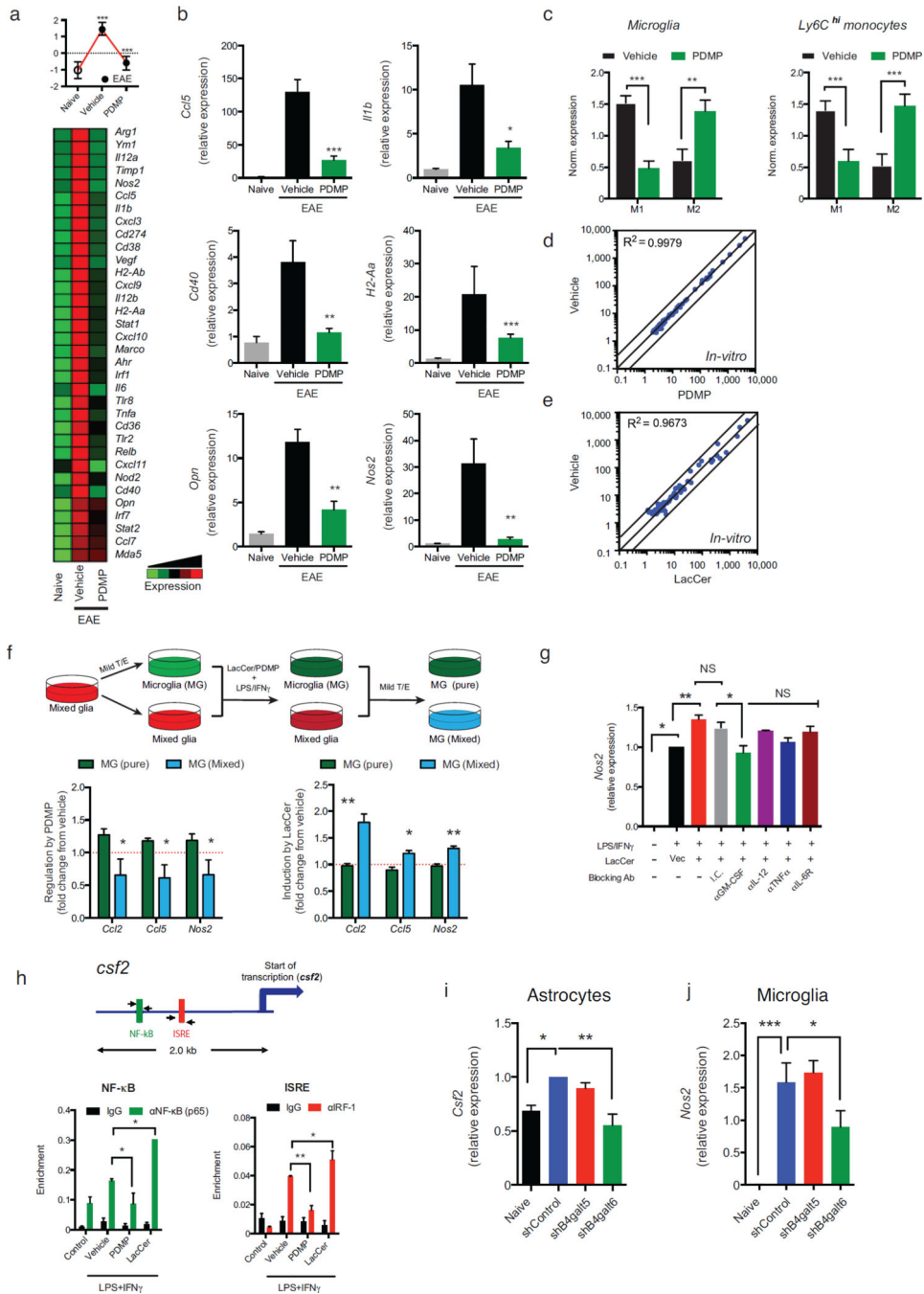
Figure 5. B4GALT6 in astrocytes regulates the activation of microglia and CNS-infiltrating monocytes

(**a**) Heatmap depicting mRNA expression, as determined by nCounter Nanostring analysis, in microglia from naïve or EAE NOD mice treated with PDMP or vehicle. Representative data of three independent experiments. Statistical analysis by Student's t-test. (**b**) qPCR analysis of *ccl5, il1b, opn, nos2, cd40*, and *H2-Aa* gene expression relative to *Gapdh*. (**c**) Mean normalized expression of genes associated with M1- or M2-phenotype in microglia (Supplementary Table 3) (**c, left panel**) and Ly6C^{high} monocytes (**c, right panel**). Statistical

analysis by Student's t-test. (**d, e**) Primary microglia were pre-treated with PDMP, LacCer, or vehicle, followed by activation with LPS/IFNγ for 6h or left un-treated (control) as in (Fig. 3a). mRNA expression was determined by nCounter Nanostring analysis (**d, e**) was determined. Representative data of five independent experiments. (**f**) Mixed glia cultures were treated with mild trypsin/EDTA (T/E) to remove the astrocyte monolayer leaving only the microglia attached to the plate, or left un-treated. Cultures were pre-treated with PDMP, LacCer or vehicle, and activated with LPS/IFNγ for 6h. Following activation, both cultures were washed, and incubated with mild T/E to remove the astrocytes; thus, leaving only the microglia (MG) attached to the plates. RNA was harvested from microglia treated in the absence [MG (pure)] or presence [MG (mixed)] of astrocytes and gene expression was analyzed by qPCR for the expression *ccl2, ccl5* and *nos2* relative to *gapdh*. Data present the relative effect of PDMP (left panel) or LacCer (right panel) pre-treatment on LPS/IFNγ-triggered gene induction, from five independent experiments. Statistical analysis by Student's t-test. (**g**) Mixed glia were pre-treated with indicated blocking antibodies or appropriate isotype controls (25μg/ml) and LacCer (10μM) or vehicle control, and then activated with LPS/IFNγ for 6h. Microglia were isolated as in (**f**), and microglial-*nos2* expression was determined by qRT relative to *gapdh* and presented as in (**f**). Representative data of three independent experiments. (**h**) ChIP analysis of the interaction of NF-κB, and IRF-1 with the *csf2* promoter in primary cultured astrocytes. (**i, j**) Expression *csf2* in astrocytes (**i**) and *nos2* in microglial cells (**j**) isolated form the CNS of chronic EAE NOD mice, 10 days after the i.c.v. injection of astrocytes-specific shRNA lentivirus as in (Fig. 3g). Data from two independent experiments. For all data, means and s.e.m. are shown. *P<0.05, **P< 0.01, ***P<0.001 and n.s. not significant.
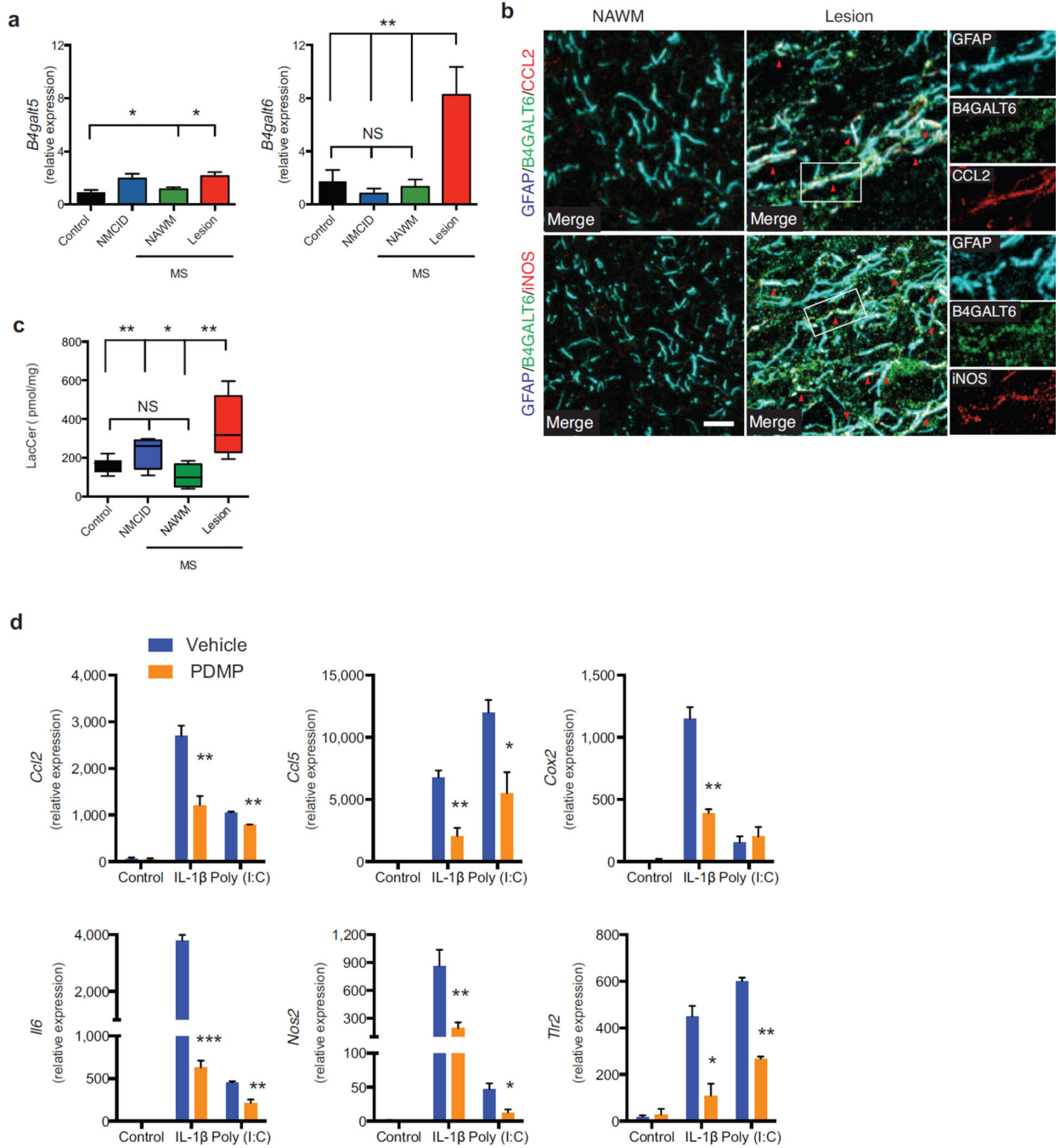
Figure 6. *B4GALT5 and B4GALT6* **and LacCer levels are up-regulated in MS lesions**
Autopsy samples were obtained from lesions (n=10) or NAWM (n=5) from MS, non-MS
CNS inflammatory diseases (NMSCID, including viral encephalitis, Rasmussen's
encephalitis and ADEM, n=5) patients and healthy controls (n=6). (**a**) qPCR analysis of
B4GALT5 and *B4GALT6* mRNA expression in CNS samples relative to *ACTB*. (**b**) IF
analysis of B4GALT6, CCL2 and iNOS in GFAP+ astrocytes in NAWM and Lesion of MS
patients. Scale Bar 10 μM (**c**) LacCer levels determined in CNS samples, relative to protein
content. Statistical analysis by one-way ANOVA, followed by Tukey post-hoc analysis. (**d**)

Primary human astrocytes were pre-treated with PDMP (25 μM) or vehicle, and activated with IL-1β (10 ng/ml) or Poly (I:C) (10 μg/ml) or left untreated (control). RNA was harvested 6h later and the expression of *CCL2, CCL5, COX2, IL6, NOS2*, and *TLR2* was analyzed by qPCR relative to *ACTB in* 3 independent experiments. Statistical analysis by Student's t-test. Data presented are mean and s.e.m. *P<0.05, **P<0.01 and ***P<0.001.